Polymer Chemistry

ROYAL SOCIETY OF CHEMISTRY

COMMUNICATION

View Article Online
View Journal | View Issue

Cite this: *Polym. Chem.*, 2020, **11**, 5974

Received 30th July 2020,
Accepted 7th September 2020

DOI: 10.1039/d0py01088j

rsc.li/polymers

Easily readable palindromic sequence-defined polymers built by cascade thiol-maleimide Michael couplings†

Qiunan Shi,[a] Xiaohuan Cao,[a] Yajie Zhang,[a] Suhua Duan,[a] Lihua Hu,[b] Yuxuan Xu,[c] Jingqiu Lu,[a] Zhihao Huang,*[a] Zhengbiao Zhang *[a,d] and Xiulin Zhu[a,e]

Palindromic sequence-induced specific and genetic functions widely exist in biological systems. Nevertheless, the study of synthetic palindromic sequence-defined polymers has received scarce attention due to the challenge of efficient synthesis. Herein, we demonstrated cascade thiol-maleimide Michael couplings (CTMMC) as an efficient chemistry to access palindromic sequences. Taking bromomaleimide as the synthon, the CTMMC enabled the construction of an array of palindromic sequences at an accelerated growth rate *via* an iterative exponential growth strategy. Moreover, owing to the synergetic cleavages of two C–S bonds located in dithiosuccinimide linkages, the palindromic sequences were easily readable (*i.e.*, decipherable) by tandem mass spectrometry. The CTMMC chemistry endowed structural versatility and diversity to the palindromic sequences, thereby uncovering many potential applications, such as anti-counterfeiting labeling and item identification like artificial "DNA".

Palindromic sequences represent a unique and important class of sequence structures, which can be deciphered in either the forward or backward direction.[1] In biological polymers, palindromic sequences have been extensively explored. For example, the double-stranded palindromic sequence repeats are often associated with the restriction endonuclease recognition site in the DNA of some bacteria. This discovery creates the fundamental of the Clustered Regularly Interspaced Short Palindromic Repeats (CRISPR) technology.[2–6] Palindromic sequences are also frequently observed in proteins as single strands, *e.g.* the palindromic region AGAAAAGA (PrP113–120) in a prion, which dictate various properties, such as increase of the binding effect, promotion of aggregation, *etc.* (Fig. 1).[7–12] Despite the fact that it is possible to create unique or improved properties/performances, man-made palindromic sequences are rarely explored due to the challenge in their synthesis.

With regard to the efficient synthesis of sequence-defined discrete polymers, the reasonable combination of an optimized synthetic strategy and efficient chemistry is crucial.[13–15] During the past years, significant progress on the synthetic strategy of sequence-defined polymers has been made, including solid-phase iterative synthesis,[16–19] template approach,[20] multicomponent reactions,[21,22] single unit monomer insertion[23,24] or even complex biomimetic molecular machines[25–27] and iterative exponential growth (IEG) strategy.[28–35] The IEG strategy (also termed the iterative convergent/divergent strategy) enabled fast chain growth in a "molecular doubling" manner. However, for the construction of defined sequences, IEG requires an efficient and orthogonal side chain installation during main chain growth.[15] On the other hand, several robust and efficient reactions have been employed in these strategies, *e.g.* copper catalyzed azide–alkyne cycloaddition (CuAAC), sulfur-fluoride exchange reaction and thiol–ene

[a]*State and Local Joint Engineering Laboratory for Novel Functional Polymeric Materials, Jiangsu Key Laboratory of Advanced Functional Polymer Design and Application, College of Chemistry, Chemical Engineering and Materials Science, Soochow University, Suzhou 215123, China. E-mail: zhhuang@suda.edu.cn, zhangzhengbiao@suda.edu.cn*

[b]*Analysis and Testing Center, Soochow University, Suzhou 215123, China*

[c]*Applied Technology College of Soochow University, Soochow University, Suzhou 215325, China*

[d]*Collaborative Innovation Center of Suzhou Nano Science and Technology, Soochow University, Suzhou 215123, China*

[e]*Global Institute of Software Technology, No. 5 Qingshan Road, Suzhou National Hi-Tech District, Suzhou 215163, China*

† Electronic supplementary information (ESI) available: Experimental details and additional characterization data. See DOI: 10.1039/d0py01088j

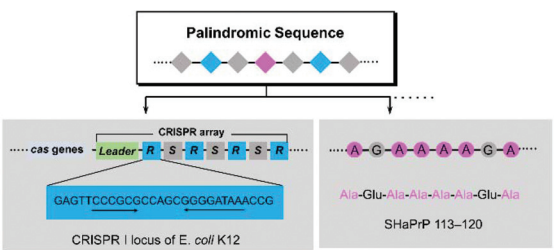

Fig. 1 Illustration of the palindromic sequences of *E. coli* K12 and *SHaPrP* 113–120, respectively.

addition.[36] To date, a typical strategy for constructing palindromic sequence-defined polymers has been bidirectional growth. By repeating the process of deprotection-coupling[37–39] or orthogonal coupling[40–42] from a double functionalized core, two uniform sequence units could symmetrically add to both sides of the precursor in one bidirectional growth cycle; thus the palindromic sequence could be realized. Besides, in 2015, Johnson *et al.* demonstrated the elegant production of a palindromic sequence by the combination of IEG with side-chain functionalization *via* CuAAC-induced chain growth.[43] The esterification or nucleophilic substitution-based side-chain functionalization enabled fast sequence construction *via* an IEG strategy. To meet sophisticated and demanding application scenarios, especially to mimic the functions of biological polymers, polymer chemists always pursue more efficient, metal-free, biocompatible and eco-friendly chemistry to access discrete and exquisite polymers. It has been well documented that thiol-maleimide Michael coupling (TMMC) is a "click" reaction which is widely used for bio-conjugation, crosslink and surface modification for biomedical materials,[44–54] owing to its mild, efficient and physiology-compatible features. In our group, TMMC together with the IEG strategy has well demonstrated its robustness and versatility in constructing discrete polymers (Scheme 1a).[55–57] For constructing symmetrical palindromic sequences, the IEG strategy could be a better option due to its exponential growth manner. Nevertheless, how to conveniently install varied side chains during fast main chain growth still remains a challenge.

It was noted that thiol and bromomaleimide could undergo cascade thiol-maleimide Michael couplings (CTMMC) in an efficient way.[58–60] Therefore, it was envisioned that bromomaleimide could successively couple with two thiols effectively, enabling both chain growth and side chain installation. Herein, by applying the IEG strategy, we demonstrated the CTMMC-enabled fast access to palindromic sequences. Through the CTMMC-integrated IEG strategy, the 1st TMMC allowed the main chain growth and the 2nd TMMC installed the pre-determined thiol-containing side chains. Variable side chains could be deliberately installed during chain growth, thus creating sequences on demand (Scheme 1b). This work opens a new way to create palindromic sequences for mimicking biological polymers and enriches the toolbox for the ultimate target of polymer synthesis, *i.e.*, the development of novel polymeric materials with superior performance.

With inherent electron deficiency, bromomaleimide (3-BrMI) can readily react with thiol *via* TMMC.[58] The reaction produced a bromide-substituted succinimide moiety, which was highly unstable and converted to maleimide by the removal of hydrogen bromide. The freshly generated male-

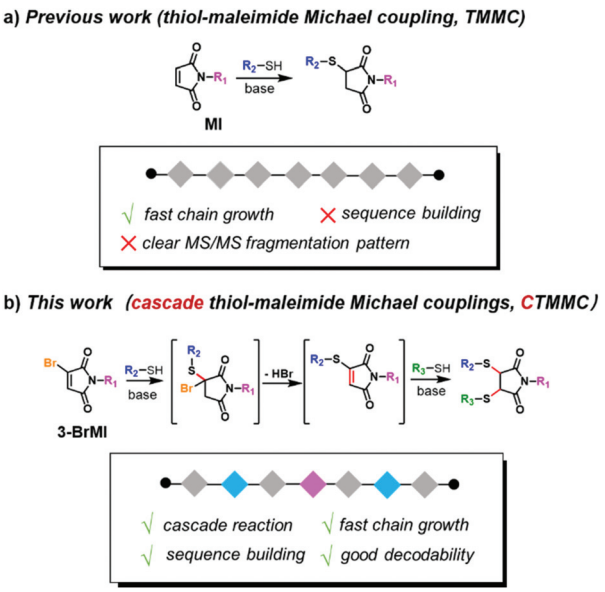

Scheme 1 (a) Previous work: discrete polymers by TMMC. (b) This work: palindromic sequences built by CTMMC.

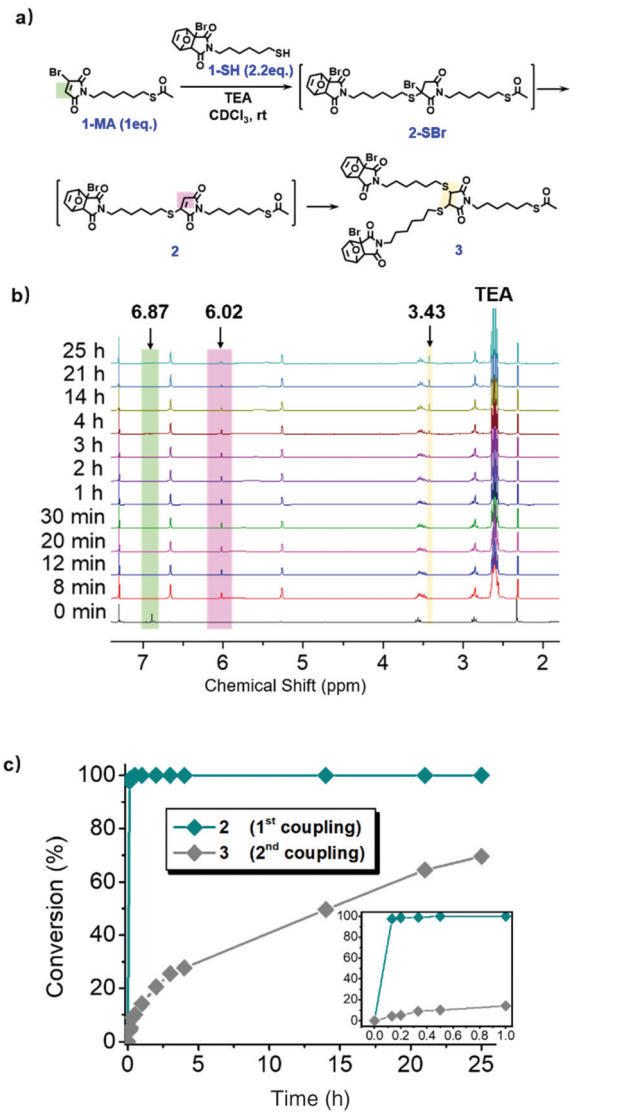

Fig. 2 (a) The schematic illustration of CTMMC. (b) *In situ* ^{1}H NMR monitoring of CTMMC (300 MHz, $CDCl_3$). (c) The kinetic plot of CTMMC in 1.0 h (inset) and 25 h.

imide was active toward the 2nd TMMC with a thiol-containing molecule, giving the dithiosuccinimide (DTS) moiety.[60] This cascade thiol-maleimide Michael couplings (CTMMC) realized the efficient installation of side chains (2nd TMMC) during main chain growth (1st TMMC). Considering the high efficiency of the cascade reaction,[61–67] CTMMC was proposed as an ideal chemistry for the construction of palindromic sequences *via* the iterative exponential growth (IEG) strategy. To verify the cascade behaviour, monomer 1 possessed a furan-protected bromomaleimide group and an acetyl-protected thiol group was designed (Scheme S1†). The orthogonal and quantitative deprotections produced the thiol-capped 1-SH and maleimide-capped 1-MA, respectively (Scheme S2 and Fig. S8, S9†), the degree of deprotection was monitored by ^{1}H NMR. The CTMMC between 1-MA (1.0 equiv.) and 1-SH (2.2 equiv.) catalysed by triethylamine was explored in deuterochloroform and monitored by NMR spectrometry (Fig. 2a). Surprisingly, the 1st TMMC was completed within only 8 min and produced intermediate 2 exclusively, determined by the disappearance of the resonance at δ 6.87 (ppm) related to 3-BrMI (marked in green, Fig. 2b). The intermediate 2-SBr was not observed due to its high activity.[68] The 2nd TMMC proceeded smoothly and afforded 3 with ~70% yield after 25 h, as determined by NMR (Fig. 2b). The reaction kinetic plots of both 1st and 2nd TMMC clearly demonstrated the cascade manner (Fig. 2c). The structures of 2 and 3 were fully confirmed by ^{1}H NMR (Fig. S10 and S11†).

Starting from monomer 1, an array of palindromic sequences was built *via* the CTMMC-integrated IEG approach. For example, as described in Fig. 2a, intermediate 2 was generated from the TMMC (iii) between 1-SH (1.2 equiv.) and 1-MA (1.0 equiv.) (Fig. 3a). After about 30 minutes of the 1st TMMC, benzyl mercaptan (B, 2.0 equiv. to ensure the conversion of the intermediate) was added *in situ* and reacted with **2** to form **B** *via* the 2nd TMMC (iv). With **B** as the precursor, repeating i to iv and using hexyl mercaptan (**A**) as the thiol agent during the 2nd TMMC (iv), the palindromic sequence of BAB was created. In the next cycle, the sequence of BABCBAB was produced by incorporating *p*-isopropyl thiophenol (C) as the thiol agent during the 2nd TMMC. By tailored installation of different thiol agents during the 2nd TMMC, other palindromic sequences of AAAAAAA, ABABABA and ABADABA were successfully created in an IEG manner, which were validated by NMR, SEC and MALDI-TOF mass spectrometry (Fig. S12–S25 and S40–S53†). Taking BABCBAB as an example, the SEC traces including its discrete precursors, *i.e.*, 2, B, BOB, BAB, BABOBAB and BABCBAB, are presented in Fig. 4a. Unimodal, symmetrical and narrow distributed SEC traces as well as an apparent molecular weight shift could be observed. The MALDI-TOF mass spectra of the discrete oligomers BOB, BAB, BABOBAB and BABCBAB are shown in Fig. 4b. A single MS peak signal agreeing well with the calculated value of the molecular mass ([M – Furan + Na]$^+$) was evidenced. The proton NMR spectrum of BABCBAB is shown in Fig. 4c. Apparently, all the characteristic resonance could be perfectly assigned to the theoretical one. Specifically, the resonance of the protons of protected species at both terminals, *i.e.*, furan and acetyl groups, could be easily identified at δ 6.64 (a), 5.26 (b) and 2.32 (g) ppm, implying the high fidelity of terminal protections. Furthermore, the complete disappearance of the proton resonance at δ 6.02 ppm

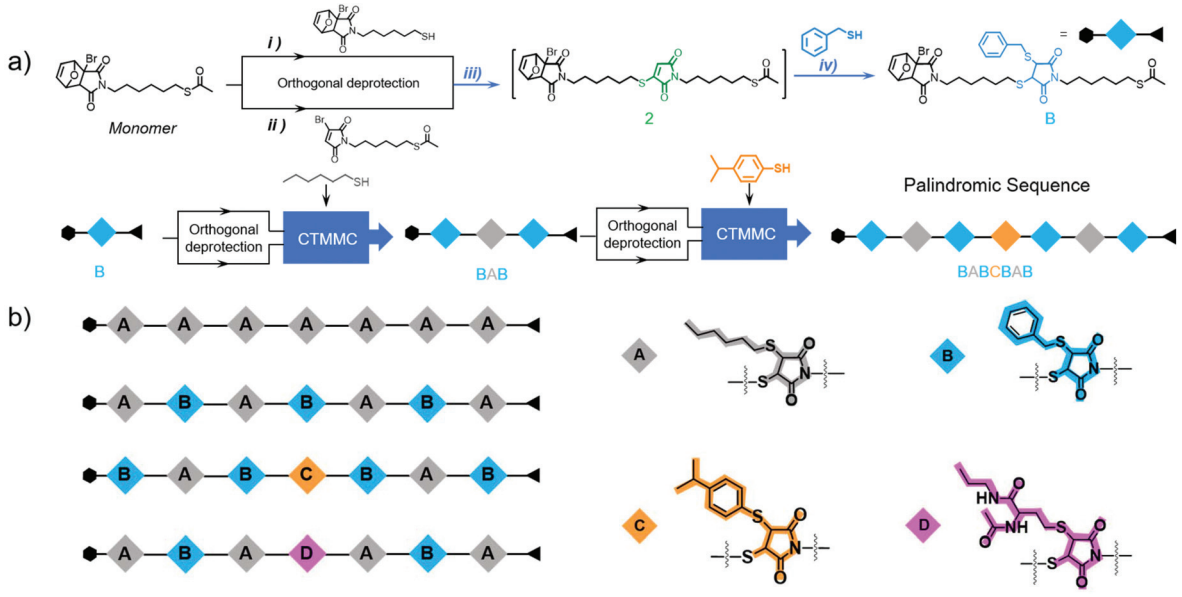

Fig. 3 (a) Synthetic illustration of the palindromic sequence constructed by the CTMMC-integrated IEG strategy, including orthogonal deprotections of thiol and 3-BrMI (i and ii) and subsequent CTMMC (iii and iv): (i) con. HCl, MeOH, 55 °C, inert atmosphere, 6–14 h, (ii) toluene, 110 °C, 8–12 h, (iii) TEA, $CHCl_3$ or THF, 25 °C, 30 min, (iv) TEA, $CHCl_3$, 25 °C, 12 h. (b) Illustration of the target palindromic sequences by installing different thiols before the 2nd TMMC in each IEG cycle. The symbol ⬢ indicates the furan-protected bromomaleimide end group, and the symbol ◀ indicates the acetyl-protected thiol end group.

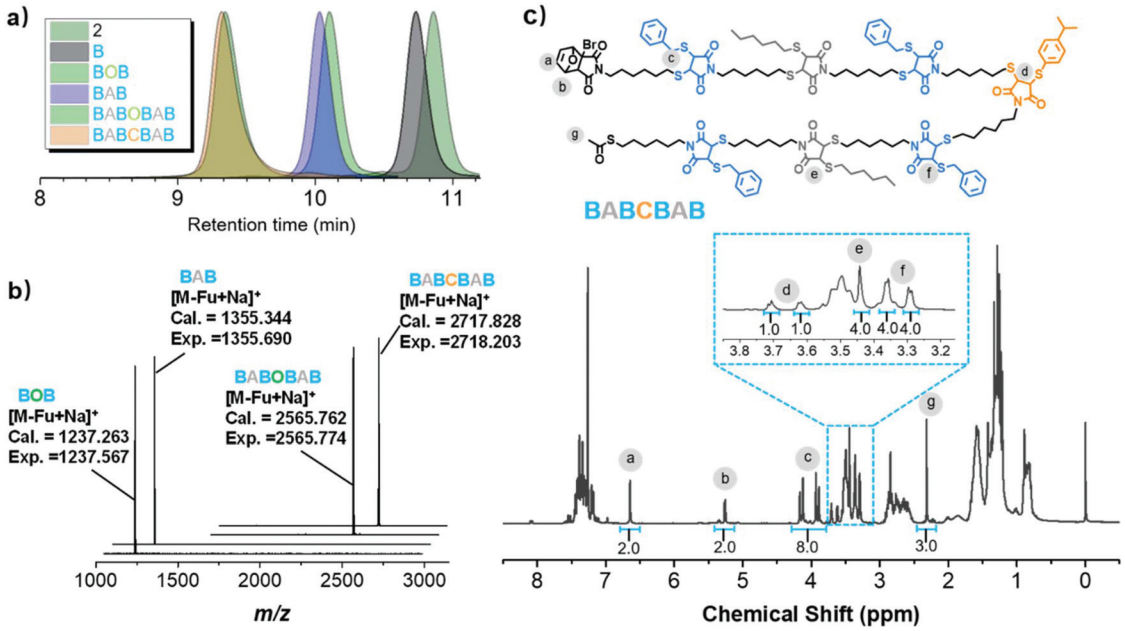

Fig. 4 (a) SEC traces of discrete precursors with palindromic sequences. THF was used as an eluent. (b) MALDI-TOF mass spectra of BOB, BAB, BABOBAB and BABCBAB. (c) The ^{1}H NMR spectrum of BABCBAB recorded in $CDCl_3$ (Bruker, 300 MHz, TMS).

belonging to the maleimide moiety resulting from the 1st TMMC indicated the success of the 2nd TMMC. The resonance between δ 3.70–3.65 (d), 3.44 (e) and 3.36–3.30 (f) ppm verified the formation of DTS through CTMMC. The results of the MALDI-TOF mass spectrometry and isolated yields are presented in Table 1 for a clear illustration. All the results confirmed the structural uniformity of these palindromic sequences, which were built in reasonable yields. It should be noted that CTMMC was not limited to the construction of palindromic sequences. We proved that more complex sequences were prepared by iterative and cross growth (Scheme S14†).

To mimic the biological palindromic sequence, the synthetic palindromic sequence should be readable or decipherable for fulfilling potential applications.[7,69] The sequencing by tandem mass spectrometry (MS/MS) is popularly considered as a versatile and valid tool to read the sequence information stored in both biological and synthetic polymers. During MS/MS sequencing, the metastable polymer chains are fragmented into many sequence-induced species upon the imposed energy, such as a pulsed electric field or inert gas collision.[70–72] The m/z analysis of the fragmented species enables the restoration of the sequence information. However, due to similar bond energies of the covalent bonds of the polymeric chain, the MS/MS sequencing frequently induced many irregular and secondary chain fragmentations, giving rise to many interfering and unattributable MS signals.[73,74] On the other hand, both fragment pieces from the cleavage of each chemical bond are detected by MS/MS, which could further perturb the sequencing process. Therefore, for "easy-to-read" and predictable MS/MS signals, the selective cleavage of chemical bonds in repeat units to afford legible sequence-related MS signals is highly desirable. For example, Lutz *et al.* cleverly incorporated wieldy C–ON alkoxyamine bonds in each repeating unit to provide a clear and easily readable MS/MS fragmentation pattern.[18,75,76] In order to probe the information readability of these palindromic sequences, the tetramers were subjected to MS/MS sequencing. Excitingly, the MS/MS spectra of tetramers showed clear fragmentation patterns, which were possibly due to the controlled cleavages on the C–S bonds of the DTS moiety (Fig. S56, S57 and Tables S2, S3†). To confirm this hypothesis, the computer calculation of the bond dissociation energy (BDE) was performed *via* the density functional theory method (Table S1†). According to the results, a synergetic cleavage mechanism was proposed (Fig. S54†). Specifically, during MALDI-TOF MS/MS sequencing, the cleavage of one C–S bond attached to the succinimide group gave rise to a carbon radical species. The driving force of stabilization causes the BDE of the adjacent C–S bond to significantly drop from 56.8 to 7.9 kcal mol^{-1}.[77] Thus, after rearrangement,

Table 1 MALDI-TOF MS characterization and yields of palindromic sequence-defined polymers

Palindromic sequence	$[M - Furan + Na]^+$ $m/z_{cal.}$ (Da)	$m/z_{exp.}$ (Da)	Error (Da)	Yield[a] (%)
AAA	1343.438	1343.856	+0.418	59.8
ABA	1349.391	1349.499	+0.108	54.7
BAB	1355.344	1355.690	+0.346	51.8
AAAAAAA	2660.031	2660.401	+0.370	33.6
ABABABA	2677.891	2678.046	+0.155	23.6
BABCBAB	2717.828	2718.203	+0.375	26.3
ABADABA	2771.965	2772.322	+0.357	18.4

[a] Isolated yield: Over a CTMMC-integrated IEG cycle (4 steps in total) and purified by column chromatography over silica gel.

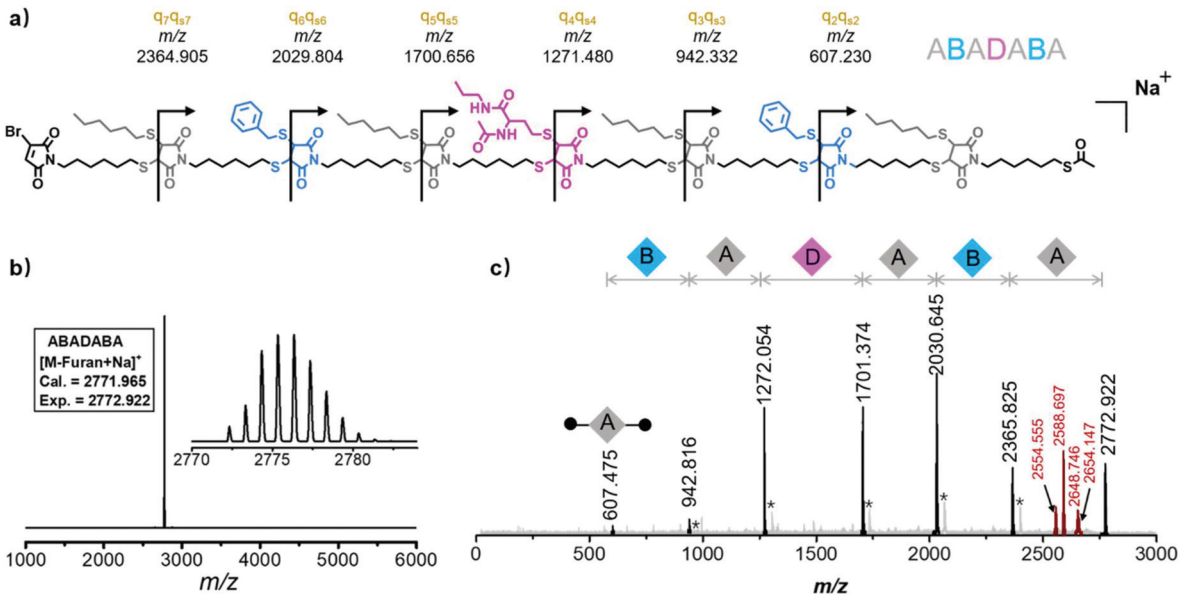

Fig. 5 (a) Illustration of the theoretical fragmentations of ABADABA. (b) The MALDI-TOF MS spectrum and (c) MALDI-TOF MS/MS spectrum of ABADABA. *Signals arise from concomitant fragmentations, detailed in the ESI (Table S7†).

a series of dominant fragments with stable maleimide terminus were observed in the tandem mass spectrum, resulting in the easy-to-read sequences.

To further validate the good decodability of these synthetic palindromic sequences, ABADABA was sequenced by MS/MS spectrometry (Fig. 5). It found that the MALDI-TOF MS/MS spectrum of ABADABA displayed a clear fragmentation pattern (Fig. 5b and c). The MS/MS-induced synergetic cleavages of the C–S bonds of DTS broke the polymer chain and led to distinct sequence-related signals in the MS/MS spectrum, *e.g.*, the first fragment at *m*/*z* 607.475 assigned to $[A\text{-}\omega + Na]^+$ (named q_2qs_2) and the homolog series of q_3qs_3 at *m*/*z* 942.816 ($[B\text{-}A\text{-}\omega + Na]^+$), q_4qs_4 at *m*/*z* 1272.054 ($[A\text{-}B\text{-}A\text{-}\omega + Na]^+$), q_5qs_5 at *m*/*z* 1701.374 ($[D\text{-}A\text{-}B\text{-}A\text{-}\omega + Na]^+$), q_6qs_6 at *m*/*z* 2030.645 ($[A\text{-}D\text{-}A\text{-}B\text{-}A\text{-}\omega + Na]^+$), and q_7qs_7 at *m*/*z* 2365.825 ($[B\text{-}A\text{-}D\text{-}A\text{-}B\text{-}A\text{-}\omega + Na]^+$) could be easily identified with the concomitant fragmentation signals ($[M + 32]^+$) marked with asterisks as shown in Table S7.† Thus, the sequence information α-A-B-A-D-A-B-A-ω could be explicitly deciphered (Fig. 5c) from the dominant and unidirectional MS/MS signals. Interestingly, the structural information of the side chain pendent on the DTS moiety could also be decoded by calculating the *m*/*z* interval with the precursor ion. For example, the *m*/*z* intervals 118.775 and 124.176 Da implied the hexyl mercaptan (A) and benzyl mercaptan (B)-derived side chains, respectively. This information could be decoded and the intervals 218.367 and 184.225 Da revealed unit D (marked in red in Fig. 5c). To demonstrate the "easy-to-read" characteristic of the palindromic sequence, a "sequence unknown" sample with a given MS/MS-induced fragmentation pattern (Table S8†) could be easily deciphered within 30 minutes. The details of the deciphering process are described in the ESI (Fig. S62†). Therefore, owing to the unique DTS moiety, the clear and unidirectional fragmentation patterns greatly facilitated the sequencing of these palindromic sequences (Tables S2–S7†). Such easily readable palindromic sequences could be used as artificial DNA for anti-counterfeit purposes.[78] As a proof-of-concept, an anti-counterfeit inkjet ink labelled by a DTS-incorporated palindromic sequence-defined macromolecule was illustrated (Fig. S63†), highlighting its good potential in anti-counterfeit applications.

Conclusions

In summary, a straightforward and efficient CTMMC combined IEG strategy was demonstrated for constructing palindromic sequence-defined polymers. This chemistry allows fast chain growth with convenient side chain installations. An array of palindromic sequences with different side chains was successfully constructed. Moreover, tandem MS sequencing provided a unidirectional, clear and predictable fragmentation pattern due to the synergetic cleavages of DTS moieties, endowing the palindromic sequence with good decodability. This work offered an example for constructing palindromic sequences by applying cascade chemistry, establishing an efficient platform for constructing precision polymers.

Conflicts of interest

There are no conflicts to declare.

Acknowledgements

This work was supported by the National Natural Science Foundation of China (21925107 and 21674072), the China

Post-doctoral Science Foundation (2020M671571), the Priority Academic Program Development of Jiangsu Higher Education Institutions (PAPD) and the Program of Innovative Research Team of Soochow University.

Notes and references

1 T. Cavalier-Smith, *Nature*, 1974, **250**, 467–470.
2 S. Al-Attar, E. R. Westra, J. van der Oost and S. J. Brouns, *Biol. Chem.*, 2011, **392**, 277–289.
3 S. Camporesi and G. Cavaliere, *Pers. Med.*, 2016, **13**, 575–586.
4 N. V. Munshi, *Circulation*, 2016, **134**, 777–779.
5 M. Naeimi Kararoudi, S. S. Hejazi, E. Elmas, M. Hellstrom, M. Naeimi Kararoudi, A. M. Padma, D. Lee and H. Dolatshad, *Front. Immunol.*, 2018, **9**, 1711.
6 C. Richter, J. T. Chang and P. C. Fineran, *Viruses*, 2012, **4**, 2291–2311.
7 K. Hettiarachchi, S. Ridge, D. W. Thomas, L. Olson, C. R. Obi and D. Singh, *J. Pept. Res.*, 2001, **57**, 151–161.
8 M. Giel-Pietraszuk, M. Hoffmann, S. Dolecka, J. Rychlewski and J. Barciszewski, *J. Protein Chem.*, 2003, **22**, 109–113.
9 V. A. Wagoner, M. Cheon, I. Chang and C. K. Hall, *Proteins*, 2011, **79**, 2132–2145.
10 N. Prasanth, M. K. Vaishnavi and K. Sekar, *J. Biosci.*, 2013, **38**, 173–177.
11 L. Thoma, E. Sepulveda, A. Latus and G. Muth, *Front. Microbiol.*, 2014, **5**, 499.
12 L. Ning, Q. Wang, Y. Zheng, H. Liu and X. Yao, *Mol. Biosyst.*, 2015, **11**, 647–655.
13 J. F. Lutz, M. Ouchi, D. R. Liu and M. Sawamoto, *Science*, 2013, **341**, 1238149.
14 J. F. Lutz, J. M. Lehn, E. W. Meijer and K. Matyjaszewski, *Nat. Rev. Mater.*, 2016, **1**, 16024.
15 S. C. Solleder, R. V. Schneider, K. S. Wetzel, A. C. Boukis and M. A. R. Meier, *Macromol. Rapid Commun.*, 2017, **38**, 1600711.
16 J. Sun, X. Liao, A. M. Minor, N. P. Balsara and R. N. Zuckermann, *J. Am. Chem. Soc.*, 2014, **136**, 14990–14997.
17 A. Al Ouahabi, M. Kotera, L. Charles and J. F. Lutz, *ACS Macro Lett.*, 2015, **4**, 1077–1080.
18 R. K. Roy, A. Meszynska, C. Laure, L. Charles, C. Verchin and J. F. Lutz, *Nat. Commun.*, 2015, **6**, 7237.
19 G. Cavallo, A. Al Ouahabi, L. Oswald, L. Charles and J. F. Lutz, *J. Am. Chem. Soc.*, 2016, **138**, 9417–9420.
20 J. Niu, R. Hil and D. R. Liu, *Nat. Chem.*, 2013, **5**, 282–292.
21 S. C. Solleder and M. A. R. Meier, *Angew. Chem., Int. Ed.*, 2014, **53**, 711–714.
22 S. C. Solleder, D. Zengel, K. S. Wetzel and M. A. R. Meier, *Angew. Chem., Int. Ed.*, 2016, **55**, 1204–1207.
23 D. Y. Oh, M. Ouchi, T. Nakanishi, H. Ono and M. Sawamoto, *ACS Macro Lett.*, 2016, **5**, 745–749.
24 Z. X. Huang, B. B. Noble, N. Corrigan, Y. Y. Chu, K. Satoh, D. S. Thomas, C. J. Hawker, G. Moad, M. Kamigaito, M. L. Coote, C. Boyer and J. T. Xu, *J. Am. Chem. Soc.*, 2018, **140**, 13392–13406.
25 B. Lewandowski, G. De Bo, J. W. Ward, M. Papmeyer, S. Kuschel, M. J. Aldegunde, P. M. E. Gramlich, D. Heckmann, S. M. Goldup, D. M. D'Souza, A. E. Fernandes and D. A. Leigh, *Science*, 2013, **339**, 189–193.
26 G. De Bo, S. Kuschel, D. A. Leigh, B. Lewandowski, M. Papmeyer and J. W. Ward, *J. Am. Chem. Soc.*, 2014, **136**, 5811–5814.
27 G. De Bo, M. A. Y. Gall, M. O. Kitching, S. Kuschel, D. A. Leigh, D. J. Tetlow and J. W. Ward, *J. Am. Chem. Soc.*, 2017, **139**, 10875–10879.
28 K. Takizawa, H. Nulwala, J. Hu, K. Yoshinaga and C. J. Hawker, *J. Polym. Sci., Part A: Polym. Chem.*, 2008, **46**, 5977–5990.
29 K. Takizawa, C. Tang and C. J. Hawker, *J. Am. Chem. Soc.*, 2008, **130**, 1718–1726.
30 S. Binauld, D. Damiron, L. A. Connal, C. J. Hawker and E. Drockenmuller, *Macromol. Rapid Commun.*, 2011, **32**, 147–168.
31 F. A. Leibfarth, J. A. Johnson and T. F. Jamison, *Proc. Natl. Acad. Sci. U. S. A.*, 2015, **112**, 10617–10622.
32 Y. Jiang, M. R. Golder, H. V. Nguyen, Y. Wang, M. Zhong, J. C. Barnes, D. J. Ehrlich and J. A. Johnson, *J. Am. Chem. Soc.*, 2016, **138**, 9369–9372.
33 M. R. Golder, Y. Jiang, P. E. Teichen, H. V. Nguyen, W. Wang, N. Milos, S. A. Freedman, A. P. Willard and J. A. Johnson, *J. Am. Chem. Soc.*, 2018, **140**, 1596–1599.
34 C. H. Ju, C. C. Meng, J. H. Ma, X. Y. Zhang and S. T. Ding, *Chem. Commun.*, 2020, **56**, 3955–3958.
35 J. M. Lee, M. B. Koo, S. W. Lee, H. Lee, J. Kwon, Y. H. Shim, S. Y. Kim and K. T. Kim, *Nat. Commun.*, 2020, **11**, 1–9.
36 C. J. Yang, J. P. Flynn and J. Niu, *Angew. Chem., Int. Ed.*, 2018, **57**, 16194–16199.
37 N. Zydziak, F. Feist, B. Huber, J. O. Mueller and C. Barner-Kowollik, *Chem. Commun.*, 2015, **51**, 1799–1802.
38 N. Zydziak, W. Konrad, F. Feist, S. Afonin, S. Weidner and C. Barner-Kowollik, *Nat. Commun.*, 2016, **7**, 13672.
39 M. Van De Walle, K. De Bruycker, T. Junkers, J. P. Blinco and C. Barner-Kowollik, *ChemPhotoChem*, 2019, **3**, 225–228.
40 W. Konrad, F. R. Bloesser, K. S. Wetzel, A. C. Boukis, M. A. R. Meier and C. Barner-Kowollik, *Chem. – Eur. J.*, 2018, **24**, 3413–3419.
41 W. Konrad, C. Fengler, S. Putwa and C. Barner-Kowollik, *Angew. Chem., Int. Ed.*, 2019, **58**, 7133–7137.
42 B. Zhao, Z. Gao, Y. Zheng and C. Gao, *J. Am. Chem. Soc.*, 2019, **141**, 4541–4546.
43 J. C. Barnes, D. J. Ehrlich, A. X. Gao, F. A. Leibfarth, Y. Jiang, E. Zhou, T. F. Jamison and J. A. Johnson, *Nat. Chem.*, 2015, **7**, 810–815.
44 L. J. Wong, M. Kavallaris and V. Bulmus, *Polym. Chem.*, 2011, **2**, 385–393.
45 T. N. Gevrek, T. Bilgic, H. A. Klok and A. Sanyal, *Macromolecules*, 2014, **47**, 7842–7851.

46 H. Moon, J. Lee, J. Min and S. Kang, *Biomacromolecules*, 2014, **15**, 3794–3801.
47 P. M. Kharkar, K. L. Kiick and A. M. Kloxin, *Polym. Chem.*, 2015, **6**, 5565–5574.
48 P. Chakma, L. H. R. Possarle, Z. A. Digby, B. R. Zhang, J. L. Sparks and D. Konkolewicz, *Polym. Chem.*, 2017, **8**, 6534–6543.
49 N. Bellassai, A. Marti, G. Spoto and J. Huskens, *J. Mater. Chem. B*, 2018, **6**, 7662–7673.
50 P. Chakma, Z. A. Digby, J. Via, M. P. Shulman, J. L. Sparks and D. Konkolewicz, *Polym. Chem.*, 2018, **9**, 4744–4756.
51 L. E. Jansen, L. J. Negron-Pineiro, S. Galarza and S. R. Peyton, *Acta Biomater.*, 2018, **70**, 120–128.
52 F. Jivan, N. Fabela, Z. Davis and D. L. Alge, *J. Mater. Chem. B*, 2018, **6**, 4929–4936.
53 J. Ramos-Soriano, J. J. Reina, B. M. Illescas, J. Rojo and N. Martin, *J. Org. Chem.*, 2018, **83**, 1727–1736.
54 Y. Zhou, Y. C. Qu, Q. Yu, H. Chen, Z. B. Zhang and X. L. Zhu, *Polym. Chem.*, 2018, **9**, 3238–3247.
55 Z. H. Huang, J. F. Zhao, Z. M. Wang, F. Y. Meng, K. S. Ding, X. Q. Pan, N. C. Zhou, X. P. Li, Z. B. Zhang and X. L. Zhu, *Angew. Chem., Int. Ed.*, 2017, **56**, 13612–13617.
56 Z. M. Wang, Z. H. Huang, N. C. Zhou, X. H. Dong, X. L. Zhu and Z. B. Zhang, *Polym. Chem.*, 2017, **8**, 2346–2352.
57 B. L. Liu, Q. N. Shi, L. H. Hu, Z. H. Huang, X. L. Zhu and Z. B. Zhang, *Polym. Chem.*, 2020, **11**, 1702–1707.
58 L. M. Tedaldi, M. E. B. Smith, R. I. Nathani and J. R. Baker, *Chem. Commun.*, 2009, 6583–6585.
59 L. Castaneda, Z. V. F. Wright, C. Marculescu, T. M. Tran, V. Chudasama, A. Maruani, E. A. Hull, J. P. M. Nunes, R. J. Fitzmaurice, M. E. B. Smith, L. H. Jones, S. Caddick and J. R. Baker, *Tetrahedron Lett.*, 2013, **54**, 3493–3495.
60 J. Youziel, A. R. Akhbar, Q. Aziz, M. E. Smith, S. Caddick, A. Tinker and J. R. Baker, *Org. Biomol. Chem.*, 2014, **12**, 557–560.
61 L. F. Tietze, *Chem. Rev.*, 1996, **96**, 115–136.
62 K. C. Nicolaou, D. J. Edmonds and P. G. Bulger, *Angew. Chem., Int. Ed.*, 2006, **45**, 7134–7186.
63 A. Padwa and S. K. Bur, *Tetrahedron*, 2007, **63**, 5341–5378.
64 K. C. Nicolaou and J. S. Chen, *Chem. Soc. Rev.*, 2009, **38**, 2993–3009.
65 Y. Wang, H. Lu and P. F. Xu, *Acc. Chem. Res.*, 2015, **48**, 1832–1844.
66 M. Porel, D. N. Thornlow, N. N. Phan and C. A. Alabi, *Nat. Chem.*, 2016, **8**, 590–596.
67 Z. Zhang, Y. Z. You and C. Y. Hong, *Macromol. Rapid Commun.*, 2018, **39**, 1800362.
68 R. Kalish, A. Smith and E. Smutny, *Tetrahedron Lett.*, 1971, **12**, 2241–2244.
69 C. Deng, X. Lv, J. Li, Y. Liu, G. Du, R. L. Amaro and L. Liu, *Biotechnol. Bioeng.*, 2019, **116**, 5–18.
70 S. M. Weidner and S. Trimpin, *Anal. Chem.*, 2010, **82**, 4811–4829.
71 C. D. Calvano, G. Ventura, M. Trotta, G. Bianco, T. R. I. Cataldi and F. Palmisano, *J. Am. Soc. Mass Spectrom.*, 2017, **28**, 125–135.
72 L. C. Nye, J. F. Hitzenberger, M. M. Roubelakis, M. Orfanopoulos and T. Drewello, *Int. J. Mass Spectrom.*, 2019, **436**, 59–64.
73 M. Porel and C. A. Alabi, *J. Am. Chem. Soc.*, 2014, **136**, 13162–13165.
74 J. A. Amalian, T. T. Trinh, J. F. Lutz and L. Charles, *Anal. Chem.*, 2016, **88**, 3715–3722.
75 C. Laure, D. Karamessini, O. Milenkovic, L. Charles and J. F. Lutz, *Angew. Chem., Int. Ed.*, 2016, **55**, 10722–10725.
76 A. Al Ouahabi, J. A. Amalian, L. Charles and J. F. Lutz, *Nat. Commun.*, 2017, **8**, 967.
77 K. S. Ding, Y. J. Zhang, Z. H. Huang, B. L. Liu, Q. N. Shi, L. H. Hu, N. C. Zhou, Z. B. Zhang and X. L. Zhu, *Eur. Polym. J.*, 2019, **119**, 421–425.
78 M. J. Altamimi, J. C. Greenwood, K. Wolff, M. E. Hogan, A. Lakhani, G. P. Martin and P. G. Royall, *Int. J. Pharm.*, 2019, **571**, 118656.